Effect of Versican G1 Domain Overexpression on Hyaluronan, Hyaluronidase-2, and Synovial Joint Formation in the Embryonic Chick

By

Kristen Nichole Andrews

June 28th, 2013

Director: Dr. Anthony Capehart

Major Department: Biology

Versican, an extracellular chondroitin sulfate proteoglycan which binds hyaluronan, has been hypothesized to play a role in synovial joint formation in the chick embryo. Several studies have shown versican to be involved in mesenchymal aggregation during limb chondrogenesis with diminished expression as later stages of limb development occur. Although expression within the cartilage model is decreased, versican is still found in a few areas including the joint interzone and perichondrium. The presence of versican along with hyaluronan in the interzone could further joint interzone formation, the process of which is still not completely understood. Previous studies showed that the hyaluronan degratory enzyme, hyaluronidase 2 (Hyal-2), was up-regulated in the developing joint by overexpression of the hyaluronan-binding G1 domain of versican, suggesting a role for versican in regulation of hyaluronan metabolism during early stages of synovial joint morphogenesis. The goal of this study was to manipulate versican and hyaluronan expression in the embryonic chick to obtain a better understanding of their interaction during synovial joint development. To study versican's function, an adenovirally-

encoded G1 N-terminal hyaluronan-binding domain was over-expressed via microinjection into the presumptive elbow joint of embryonic chicks. To examine the potential interaction of versican with the hyaluronan pathway during joint development, microinjection of dominant negative CD44 adenovirus, the hyaluronan synthesis inhibitor 4-methylumbelliferone, and two hyaluronidase2 shRNA viruses (hyal2-702 and hyal2-1130) with or without co-injection of adeno-G1 versican was performed. After injection, changes in expression of hyaluronan were observed via histochemistry at early cavitation stages (HH35/36). Morphological changes in the developing joint were observed using whole mount Alcian blue histochemistry and histochemical/immunocytochemical examination of tissue sections. To investigate whether adeno-G1 versican effects were dependent on hyaluronan or CD44, hyaluronan ELISA was performed to assess its accumulation due to up-regulation of Hyal-2. Overexpression of versican G1 in the developing synovial joint led to an enlargement of the interzone area and increased hyaluronan staining was seen in areas of adeno-G1 infection within treated limbs in comparison to controls. Treatment with 4-methylumbelliferone in conjunction with adeno-G1 also resulted in an increased interzone area but an overall decrease in hyaluronan accumulation. Hyaluronan ELISA results demonstrated reduced hyaluronan levels in the 4-methylumbelliferone treated samples in comparison to adeno-G1 alone. Immunohistochemical/histochemical staining along with trends seen from real-time PCR analysis of Hyal-2 suggests that the ability of G1 versican overexpression to upregulate Hyal-2 is dependent on hyaluronan.

Effect of Versican G1 Domain Overexpression on Hyaluronan, Hyaluronidase-2, and Synovial Joint Formation in the Embryonic Chick

A Thesis

Presented to

The Faculty of the Department of Biology

East Carolina University

In Partial Fulfillment

Of the Requirements for the Degree

Masters of Science in Cell Biology

By

Kristen Nichole Andrews

June 28th, 2013

Effect of Versican G1 Domain Overexpression on Hyaluronan, Hyaluronidase-2, and Synovial Joint Formation in the Embryonic Chick

By

Kristen Nichole Andrews

Approved By:

DIRECTOR OF THESIS: _____

Anthony Capehart, Ph.D.

COMMITTEE MEMBER: _____

Paul Hager, Ph.D.

COMMITTEE MEMBER: _____

Warren Knudson, Ph.D.

COMMITTEE MEMBER: _____

Baohang Zhang, Ph.D.

CHAIR OF THE DEPARTMENT OF BIOLOGY: _____

Jeff McKinnon, Ph.D.

DEAN OF THE GRADUATE SCHOOL: _____

Paul Gemperline, Ph.D.

Acknowledgements

First of all, I would like to thank Dr. Capehart for encouraging me to join the graduate program here at East Carolina University. I would like to thank him for all of his advice, patience, and guidance throughout the years. Everything that he did was greatly appreciated and has helped mold me into a better researcher.

Much thanks also goes to the Department of Biology at East Carolina University. Thank you for acceptance into the program as well as for providing a facility to complete my research as well as the opportunity to teach undergraduate labs and for funding throughout the years.

I would also like to thank all of the members on my thesis committee: Dr. Warren Knudson, Dr. Paul Hager, and Dr. Baohong Zhang. All of my committee members were very encouraging and helpful throughout my project. I would like to especially thank Dr. Knudson and the members of his lab for their help and also for allowing me to come into their lab and use their materials to complete some of the work involved in this project. Although he was not a member of my thesis committee, I would also like to extend a thank you to Dr. Eric Anderson who helped me with the PCRs and qRT that I performed.

Finally, I would like to thank all of my family and friends that have supported me and helped me throughout these past few years. Thank you to Partha Nagchowdhuri, a former graduate student, that helped me learn all the methods used in this project, especially microinjections. Thanks to my many close friends including Alexis Bass, Caitlin Burklew, Matthew Bishop, Erika Tlsty,

and Jacob Hill for keeping me sane throughout my stressful moments. Thanks to my wonderful dog, Ruutu, who has always been there to welcome me home with a wagging tail and a loving heart. A special thank you to my parents, Philip and Vickie Andrews, who have been more than supportive and have kept me going through the rough times over the last three years, I love you both and could not have completed this degree without your words of wisdom and love.

Table of Contents

List of Tables

List of Figures

1. INTRODUCTION

Limb Development

Limb development is an unresolved research question in biology. The chick limb bud begins to form about 3 days into development, also known as HH17 (Hamburger and Hamilton 1951). From HH17 until HH21 the developing limb includes an accumulation of mesodermal cells that are very uniform morphologically; these cells are surrounded by ectoderm (Knudson et al., 1985). The next stage occurs as cell condensation takes place and mesodermal cells pack together and differentiate into chondrocytes. The condensation of pre-cartilage mesenchymal cells is a necessary process for overall chondrogenesis in the developing vertebrate limb and these cells undergo aggregation in a proximal to distal direction (Hall and Miyake, 1992, 2000; Shepard et al., 2007). While this condensation of mesenchymal cells is taking place, increased levels of versican, tenascin, fibronectin, and other cell surface and ECM molecules are expressed (Hall and Miyake, 1992; Snow et al., 2005; Shepard et al., 2007; Choocheep et al., 2010). Aggregated mesenchymal cells are led to differentiate into chondrocytes by BMPs (bone morphogenetic proteins) and other growth factors, such as GDF-5 and TGF-β (Choocheep et al., 2010). Different genes have been found to play roles in chondrogenesis including Sox9; a study performed in mouse embryos found that Sox9 expression was upregulated before and during chondrogenesis and if interrupted, mutations involving the Sox9 gene led to skeletal deformations and dysplasia (Foster et al., 1994; Wagner et al., 1994; Bell et al., 1997; Ng et al., 1997). Collagen type II has also been identified as a large component of cartilage that helps to maintain the overall structure and is regulated by Sox9 (Bell et al., 1997; Ng et al., 1997). Aggrecan, a chondroitin sulfate proteoglycan, is also a major component and has the ability to bind and interact with hyaluronan (Hardingham et al., 1972; Knudson et al., 2001) which gives

hyaline cartilage its characteristic properties. The actual onset of synovial joint development occurs when the interzone begins to appear. This interzone has three layers, two outer layers near the future epiphyseal ends of long bone rudiment, which will contribute to the articular cartilage of the opposing proximal and distal ends, and a third layer that is a thin intermediate zone which will eventually form the fluid-filled synovial cavity (Ito and Kida, 2000; Guo et al., 2004; Pacifici et al., 2005). Interzone formation is characterized by the grouping and flattening of mesenchymal cells (Pacifici et al., 2005). Different growth factors, signaling molecules, transcription factors and other regulatory molecules are expressed during the formation of the interzone including several members of the Wnt family such as Wnt-9a, Wnt-16, and Wnt-4 that transduce their signals through the canonical Wnt pathway (Guo et al., 2004).

The next step in joint development is cavitation; this occurs when the proximal and distal region of the forming joint separate and the synovial cavity is formed. The cavitation process has been linked to the accumulation of hyaluronan and one of its cell surface receptors, CD44. Hyaluronan and CD44 are thought to destabilize tissue integrity of the central interzone and lead to the actual separation of the joint sides (Craig et al., 1990; Archer et al., 1994; Edwards et al., 1994; Pitsillides et al., 1995). Knockout of HAS2, a major hyaluronan synthase, in a mouse model resulted in deformed limbs as well as malformed or absent joints, implicating hyaluronan's importance in joint cavitation (Matsumoto et al., 2009). Joint morphogenesis is another process that occurs following cavitation and is the least understood. During morphogenesis the two sides of the separated joints are shaped and able to interlock after the process is complete. The interlocking shapes are formed when the distal side starts to obtain a convex shape and the opposing proximal side becomes concave (Pacifici et al., 2005). By the end of synovial joint morphogenesis, the entire joint capsule has formed, including the fluid-filled

synovial cavity and the articular cartilages. Versican, a large chondroitin sulfate proteoglycan, has been found to play an important role during early stages of skeletal formation and continues to be expressed within articular cartilage and synovial tissue after morphogenesis is complete (Snow et al., 2005; Shepard et al., 2007).

Versican

Versican is a chondroitin sulfate proteoglycan of the hyalectin family found within the extracellular matrix (ECM). Versican is expressed constitutively in adult tissues such as the heart, blood vessels, and brain and transiently in developing tissues such as hair follicles, developing heart, and pre-cartilage mesenchymal condensations of the limb skeletal primordium (Bode-Lesniewska et al., 1996; Kimata et al., 1984; Shimomura et al., 1990; Snow et al., 2005; Williams et al., 2005; Choocheep et al., 2010). The transient expression of versican within areas where cells are accumulating suggests that this molecule is an important factor in cell aggregation that will eventually lead to tissue morphogenesis (Choocheep et al., 2010; Williams et al., 2005; Shepard et al., 2008). The ECM assists in control of cell behavior and phenotype during limb chondrogenesis (Shepard et al., 2007; Knudson et al., 1985) and evidence suggests that versican participates in these activities. Based on studies of versican expression patterns and effects on cell behavior in vitro, versican is believed to regulate the function of ligands within the ECM that may control signaling leading to cartilage development and synovial joint formation (Snow et al., 2005; Shepard et al., 2007; Choocheep et al., 2010). Many studies have supported the idea that versican can interact with other extracellular matrix molecules, such as fibronectin, to allow individual cells to come together to form aggregates (Williams et al., 2005; Kamiya et al., 2006; Choocheep et al., 2010). Versican has also been reported to participate in other

important morphological processes including cell migration, differentiation, and proliferation (Yamagata 1989, Zhang et al., 1999; Zhang et al., 1998; Zhang et al., 2001).

Versican contains three different domains, G1, G2, and G3. The N-terminal G1 domain includes an immunoglobulin-like repeat followed by two link protein-like motifs necessary for interactions with hyaluronan (Kimata et al., 1986; Zimmerman and Rouslahti, 1989; Ang et al., 1999; Yang et al., 1999; Zhang et al., 1999). The G2 domain is comprised of two chondroitin sulfate glycosaminoglycan attachment regions (GAG-α and –β) encoded by differentially spliced exons that produce four isoforms, V0-V3. The third domain, G3, consists of two EGF repeats, a C-lectin like region and regulatory motif that appears important for cell and matrix interactions (Wu et al., 2005).

The V0-V3 isoforms formed from alternative splicing of GAG-encoding domains are found within different tissues (Shinomura et al., 1993). The V0 isoform contains both GAG-α and -β regions. The V1 isoform includes only the GAG-β attachment region while the V2 isoform consists of only GAG-α. The V3 isoform only contains the G1 and G3 domains of versican and does not contain either GAG attachment region (Zimmerman and Rouslahti, 1989; Zako et al., 1995). The V0-V3 isoforms have been identified in tissue specific locations and may control cell behavior during migration and adhesion (Kimata et al., 1986; Zimmerman and Rouslahti, 1989; Zako et al., 1995). The V0/V1 isoforms are widely expressed including appearance in appendicular precartilage condensations and interzone of presumptive synovial joints (Snow et al., 2005; Capehart 2010). The V2 isoform is expressed predominantly in the nervous systems; however, the V3 isoform has not been detected as a protein (Choocheep et al., 2010) and there is still little known regarding its expression or function in the developing limb (Hudson et al., 2010).

The primary focus of this study was to overexpress the G1 domain of versican and study its effects on synovial joint formation in the chick embryo, especially within the interzone of the developing elbow joint. Our hypothesis was that joints injected with adeno-G1 versican would result in an overall enlargement of interzone area due to an increased accumulation of hyaluronan due to upregulation of the G1-domain. In a previous study, versican was localized within the interzone and epiphyses of the chick synovial joint supporting the idea that versican plays a part in formation and/or maintenance of the joint interzone (Shepard et al., 2007; Nagchowdhuri et al., 2012). Versican has also been located in the epiphyseal ends of long bones and perichondrium (Shinomura et al., 1990; Yamamura et al., 1997; Shepard et al., 2007) of the chick as well as within the presumptive joints of mice (Shibata et al., 2003; Snow et al., 2005). Additional evidence has been provided that suggests versican plays a role in adhesion and migration due to the pericellular matrix that is formed around the cell by interaction with hyaluronan (Wu et al., 2005). Indeed a recent study involving knockdown of versican within the chick synovial joint resulted in significant decreases in interzone area suggesting that versican is involved in creation and/or maintenance of this tissue (Nagchowdhuri et al., 2012). Additionally, versican-G1 overexpression within the developing chick elbow has revealed upregulation of several hyaluronan pathway genes, including the hyaluronidase, Hyal-2 (Vick 2012), so it was important to determine if G1-mediated upregulation of Hyal-2 was dependent on hyaluronan and/or CD44. Evidence of proteolyzed versican during synovial joint formation was found in mouse limbs during a recent study (Capehart 2010). This proteolyzed versican may allow versican fragments containing the G1 domain to be freed from the intact proteoglycan in the ECM that could further participate in joint development. In addition, versican has been shown to be co-localized with hyaluronan during early interzone formation which suggests that hyaluronan

may interact with versican's G1 domain (Matsumoto et al., 2003; Capehart 2010). Concomitant with the ability to bind hyaluronan, V0/ V1 versican may provide a mechanism that aids accumulation of hyaluronan in close association with the cell membrane that could create a stable pericellular matrix and contribute to cell adhesion and/or interzone stability during the earlier stages of limb development (Capehart 2010). When cell separation begins during cavitation of the joint interzone there is also an increased accumulation of hyaluronan. It is possible but still unclear if versican cleavage and presence of the resulting G1-containing fragment has the capability of releasing hyaluronan from its usual CD44-mediated association with the cell surface and other ECM molecules (Capehart 2010) or if it facilitates hyaluronan interaction with CD44 or perhaps other hyaluronan receptors. This interaction of versican with hyaluronan and CD44 may be important for synovial joint formation.

Hyaluronan

Hyaluronan, a large non-sulfated glycosaminoglycan, can be found in the pericellular and extracellular space of most vertebrate tissues (Knudson et al., 2002; Kultti et al., 2009). Synthesis of hyaluronan and its degradation are believed to play a crucial role in joint cavity formation and have been shown to help establish and maintain spaces during embryonic development (Pratt et al., 1975; Pitsillides et al., 1995). This glycosaminoglycan contains charged residues that allow it to host many water molecules and also enables it to occupy a large amount of space (Sherman et al. 1994). In conjunction with other ECM components, such as aggrecan, hyaluronan can carry out many functions including formation of the basic structural unit of cartilage and may serve as a lubricant in synovial fluid (Sherman et al. 1994).

Hyaluronan can work concomitantly with cell surface receptors to promote important processes such as cell proliferation, migration, and intracellular signaling (Sherman et al., 1994; Li et al., 2007). The ability of these functions and others is dependent on degradation and regulation of hyaluronan synthesis (Sherman et al. 1994). Hyaluronan is synthesized in the plasma membrane via three different synthases, HAS1, 2, and 3. HAS2 has been shown to be the most important and is expressed in the vertebrate limb (Knudson 2003; Li et al., 2007). These synthases use UDP sugars as substrates to couple glucuronic acid and N-acetylglucosamine into a linear polymer (Kultti et al., 2009).). UDP-glucose is converted by uridine diphosphoglucose dehydrogenase (UDPGD) into the UDP-glucuronate required for the synthesis of hyaluronan (Pitsillides et al., 1995).

Before pre-cartilage condensation occurs in limb morphogenesis, cells are surrounded with an extensive ECM where hyaluronan is the main glycosaminoglycan present (Knudson et al., 2001). The overall amount of hyaluronan synthesized before the condensation event is increased compared to the amount seen during differentiation of these mesodermal cells (Knudson et al., 1985; Shambaugh et al., 1980; Toole 1972). This decrease in hyaluronan along with increased expression of other ECM/cell surface factors could be responsible for condensation in the developing limb. Hyaluronan was also found along the joint line during the time when cavitation first occurs using a biotinylated hyaluronan-binding region link-protein complex (Craig et al., 1990; Pitsillides et al., 1995) supporting the idea that hyaluronan could be made and secreted into presumptive joint space (Oster et al., 1985; Laurent 1989). These studies also supported the idea that the absence of collagen in the presumptive cavity could possibly allow hyaluronan to achieve its swelling potential. Studies have shown that a higher UDPGD activity exists in the interzone area prior to and throughout separation of the cartilaginous

elements. In addition, levels of hyaluronan synthase were also higher in these areas. This increase in activity of both UDPGD and hyaluronan synthase suggest that the cells lining sites of joint cavitation have the ability to increase hyaluronan accumulation and this could be pertinent for synovial joint formation (Pitsillides et al., 1995). A recent study that knocked out the HAS2 gene in mice resulted in a variety of phenotypes with extremely distorted limbs as well as defects in synovial cavity formation which further supports the importance of hyaluronan in overall limb development (Matsumoto et al. 2009). It is believed that hyaluronan is responsible for encouraging joint cavitation to occur via cell separation due to an action involving saturation of the hyaluronan receptor, namely CD44 (Toole 1991; Edwards et al., 1994; Pitsillides et al., 1995; Dowthwaite et al., 1998; Dowthwaite et al., 2003).

CD44

Joint interzone formation has been shown to be concomitant with an increase in synthesis of hyaluronan and also with elevation of hyaluronan-binding proteins such as CD44 (Craig et al., 1990; Edwards et al., 1994; Pitsillides et al. 1995; Dowthwaite et al., 1998; Dowthwaite et al., 2003). CD44 is a cell-surface glycoprotein that can exist in numerous isoforms via differential alternative splicing; currently several dozen isoforms are well known and all of them contain an amino terminal domain similar to cartilage link proteins (Bajorath et al., 1998; Naor et al., 2003). CD44 is capable of interacting with many extracellular and cell-surface ligands, the most important and most relevant to this study is hyaluronan (Naor et al., 2003). One possible reason for the interaction of hyaluronan with CD44 could possibly be to anchor the cells to the ECM. CD44 is a hyaluronan receptor that mediates systemic uptake and degradation of hyaluronan (Knudson et al., 2002). However, the ability of CD44 to actually bind hyaluronan is strictly

regulated since CD44 can exist in an inactive (non-binding) form and an active (binding) form (Isacke et al., 2002). The conversion of active or inactive forms is determined by changes in CD44 glycosylation, clustering in the plane of the membrane, modulation by the cytoplasmic domain, and insertion of variant exons (Isacke et al., 2002). There are at least four functional CD44 domains that can be described, extracellular distal, extracellular proximal, transmembrane, and intracellular domains. The extracellular domain of CD44 can undergo both O-linked and N-linked glycosylation and is also subject to the addition of chondroitin sulfate side-chains (Isacke 1994). The extracellular distal domain of CD44 consists of four basic amino acids that are important for the ability to bind hyaluronan (Bajorath et al., 1998; Knudson et al., 2002). CD44's extracellular proximal domain is the main location for addition of glycosaminoglycan side chains and the main area where alternative splicing variation among the different isoforms occurs (Knudson et al., 2002). The transmembrane domain of CD44 is similar to most single-pass plasma membrane proteins and accessory proteins within the lipid bilayer or associated lipids could control the functionality of CD44 (Isacke 1994; Liu and Sy 1996; Knudson et al., 2002). The associations of cytosolic proteins within the 70-amino acid intracellular domain of CD44 are believed to be responsible for the cellular control of CD44 function (Knudson et al., 2002). CD44 is believed to play an important role in cell adhesion and migration events and has also been found to be an important factor during synovial joint formation (Isacke et al., 2002). Before the cavitation process occurs, the interzone area and future articular surfaces express CD44. Within the articular surfaces there is UDPGD activity and expression of HAS and other HAS-associated molecules. However, in the interzone area there is very little UDPGD activity but there is unbound or free hyaluronan present. Once cavitation has occurred, the formed cavity is largely composed of free hyaluronan. The synovium and articular surfaces bind hyaluronan and

express CD44; these two areas also maintain HAS expression and UDPGD activity (Dowthwaite et al., 2003). Overall, the interaction of CD44 and hyaluronan plays crucial roles in events such as cell adhesion, de-adhesion, creation of cell-free spaces, and regulation of cell migration; however, there are still questions regarding signaling regulation and if these mechanisms are also used to regulate binding of this protein to other ECM ligands or in other CD44-mediated cell:cell interactions (Isacke 1994; Sherman et al., 1994). There are also still mysteries regarding CD44 participation in degradation of hyaluronan even though anti-CD44 monoclonal antibodies are capable of blocking uptake of hyaluronan but the rate and amount of hyaluronan internalization are not always consistent with a receptor-mediated mechanism (Isacke 1994).

Hyaluronidase 2

Hyaluronidases are important factors for catabolism and degradation of hyaluronan. The Hyal-2 gene has been shown to be involved in many activities including embryonic development but there is still little known regarding its regulation (Lepperdinger et al. 2001; Chow et al. 2005). Hyaluronidases are representative of a family of β-endoglucosidases that cleave internal β-1, 4 linkages resulting in the degradation of hyaluronan (Chow et al., 2006). There have been several hyaluronidase genes found in humans organized in groups of three at two different chromosomal locations (Csoka et al., 2001; Chow et al., 2005; Chow et al., 2006). Hyal-2 is found on the 3p21.3 chromosome along with Hyal-1 and Hyal-3 (Chow et al., 2005; Chow et al., 2006). Hyal-1 and Hyal-2 are the most important mammalian hyaluronidases within somatic tissues (Csoka et al., 2001; Knudson 2003) and are believed to work together to degrade hyaluronan (Csoka et al., 1999; Chow et al., 2006). Cartilage has been known to express Hyal-1, Hyal-2, and Hyal-3 transcripts (Flannery et al., 1998; Chow et al., 2005). The Hyal-2 gene has the ability to

hydrolyze hyaluronan into smaller fragments and is primarily found in lysosomes, giving this hyaluronidase interesting substrate specificity; the most efficient activity of this hyaluronidase occurs at a pH of 4.0 (Lepperdinger et al., 1998; Chow et al., 2006). A study using chick embryo fibroblasts found two hyaluronidase enzymes, cell associated and medium associated forms (Orkin et al. 1980). These enzymes appear to be lysosomal and it is believed that they are initially transported from the Golgi apparatus to the plasma membrane where they are reinternalized or secreted (Neufeld et al. 1977; Orkin et al. 1980). This suggests that the hyaluronidase is subjected to a neutral pH then integrated into a more acidic pH in the secondary lysosome (Orkin et al. 1980b). The secreted hyaluronidase is more stable at a neutral pH, unlike the intracellular form which is stable at lower pHs, possibly due to the presence of sialic acid (Orkin et al., 1980a).

There is evidence supporting a two-step process to intracellular hyaluronan degradation. First, hyaluronan is broken down from its large mass into smaller fragments by Hyal-2 at the cell surface and transported to lysosomes where Hyal-1 and β-glucuronidase and β-N-acetylglucosaminidase will continue the degradation process (Stern 2003). However, in an embryonic study involving *Xenopus laevis* there is a Hyal-2-like hyaluronidase both attached to the cell surface and intracellular; the cell surface Hyal-2 was attached via a GPI-anchor and degradation of hyaluronan occurred at both normal physiological and a more acidic pH (Mullegger et al., 2002). Another study also found evidence that Hyal-2 works intracellularly by locating recombinant C-terminal and N-terminal tagged Hyal-2; the C-terminus would not have been seen if a C-terminal cleavage had occurred in order to transfer the Hyal-2 to a GPI-anchor (Chow et al., 2006). Studies have shown that chloroquine, a lysosomotropic agent, blocks the degradation of hyaluronan into small pieces by chondrocytes (Hua et al., 1993; Chow et al.,

2005). This blockage indicates that hyaluronan is catabolized intracellularly via lysosomal hyaluronidases (Chow et al., 2005). There are clearly still unsettled issues regarding whether Hyal-2 functions intracellularly or on the cell surface; this could be dependent on state of development, and possibly cell type.

Experimental Objectives

In a recent study, a proteolyzed fragment of versican containing the G1 domain of versican was localized to the developing joint at stages immediately preceding and during cavitation (Capehart 2010), therefore, it was important to determine if the G1 domain of versican has biological activity during joint formation that could be demonstrated by adenoviral-mediated overexpression in vivo. Since recent microarray and real-time PCR work in our lab demonstrated upregulation of Hyal-2 due to overexpression of G1-versican in developing chick joint tissues (Vick 2012), it was also of interest to investigate the means by which Hyal-2 upregulation occurred. As versican, hyaluronan, and CD44 have all been found co-localized in the embryonic joint (Wu et al. 2005) and all appear to play important roles in joint formation we decided to investigate if G1-mediated upregulation of Hyal-2 was dependent on hyaluronan and/or CD44. In order to determine if G1-mediated signaling was dependent on hyaluronan, 4-methylumbelliferone was co-injected with an adenoviral-G1 domain construct. To determine if signaling was dependent on CD44, an adenovirus encoding a tailless CD44 that blocks wild-type CD44 hyaluronan interactions was co-injected with adeno-G1. Whole mount and histochemical staining of tissue sections in addition to real-time PCR, hyaluronan zymography, and hyaluronan ELISA were utilized in order to draw conclusions regarding how G1 versican-mediated signaling may occur.

2. METHODS

Embryos

Eggs (Charles River) used were viral-free and fertilized. Eggs were kept in a humidified incubator at 37.5°C until experimental treatment and subsequent harvest for analysis (AUP approval letter, Appendix A). Embryos were removed at HH 35/36 (day 9 or 10). After removal of membranes and rinsing embryos with phosphate buffered saline (PBS) they were fixed immediately in 4% paraformaldehyde.

Adenoviruses and Chemical Reagents

Replication incompetent recombinant adenoviruses (Adeno-X System, Clontech) were utilized for microinjection and used as a vector to transfer DNA to target cells of the chick limb in ovo. Genes needed to replicate the virus were removed and replaced with a cloning site that allowed insertion of recombinant DNA encoding the G1 versican domain or other constructs. When viruses bind to an integrin and are internalized, constitutive viral expression is regulated by the cytomegalovirus (CMV) promoter. Versican adenoviruses used in this study consisted of a C-terminal hemaglutinin (HA)-tagged murine G1 domain produced using bases 154-1219 (NM_001081249; Kern et al., 2007; Hudson et al., 2010). LacZ encoding adenovirus was also used in conjunction with adeno-G1 to aid in rapid identification of infected tissues (Kern et al., 2007; Hudson et al., 2010). In addition to lacZ and G1 viruses, microinjection with dominant negative adeno-CD44 (DN-CD44) (a kind gift provided by the Knudson lab) and also two hyal2 shRNA-encoding viruses (hyal2-702 and hyal2-1130), targeting HYAL-2 (XM 4142580) bases

GCAACTCTGGGGGTATTAC and TCAAGGATTATATGGAAGG respectively, were used to examine if disruptions in joint development or hyaluronan localization occurred.

Selected embryos were also injected with 4-methylumbelliferone in combination with adeno-G1 versican. Four-methylumbelliferone (4-MU) has been shown to inhibit hyaluronan synthesis since active glucuronidation of 4-MU creates large amounts of 4-MU-glucuronide resulting in the decrease of the cellular UDP-GlcUA pool (Kultti et al., 2009). Studies have also shown that 4-MU may target HAS substrate, HAS2, and possibly HAS3 (Kultti et al., 2009).

Microinjections

Eggs at 4.5 days (HH25) of incubation were cleaned using 70% ethanol, and "windowed" by removal of a small portion of the egg shell to gain access. The overlying vitelline membrane was carefully peeled away using a tungsten needle. The embryo develops on its left side which leaves the right wing exposed. The right limb was positioned and injected with recombinant adenoviruses using a pneumatic picopump (PV820 World Precision Instruments). The injection was performed by positioning the microinjection capillary needle at an approximately 45° angle anterior to the center of the wing bud. Once the capillary needle was in position the needle was inserted and approximately 1.0μL of adenovirus solution was injected. Injections of G1-adenovirus ($9.0x10^9$ ifu/ml) and DN-CD44 adenovirus ($5x10^9$ ifu/ml) were performed in a 1:1 ratio with lacZ adenovirus ($5.3x10^9$ ifu/ml) so that β-galactosidase staining could be used to monitor infection site. Other viruses and reagents used included the two hyal2 shRNA viruses ($5.0x10^9$ ifu/mL) and 4-methylumbelliferone. Four-methylumbelliferone (Sigma) was prepared at 2mM concentrations in PBS and sterilized using a 0.22μM non-pyrogenic syringe filter. Four-methylumbelliferone was co-injected with adenoviral constructs in equal amounts yielding final

concentrations of 0.5-1.0 mM dependent upon combinations utilized (adeno-G1 or adeno-G1&lacZ). Once injected, eggs were sealed with tape and returned to the incubator until the desired stage of development (HH35/36, 9 or 10 embryonic days).

Whole Mount Alcian Blue Staining

Whole mount Alcian blue staining was used to view gross morphological changes in limbs of chick embryos using a modification of Kuczuk and Scott (1984). When harvested, embryos were fixed in 4% paraformaldehyde for 40 minutes and washed in PBS before placing in 95% ethanol overnight. The next day embryos were placed in Alcian Blue stain (Sigma; prepared as 80mL 95% ethanol, 20mL glacial acetic acid, 15mg Alcian Blue, filtered before use) overnight at room temperature and rocked gently. Embryos were then rinsed twice with 95% ethanol for 1 hour each to remove remaining Alcian Blue. After rinsing, embryos were macerated in 2% potassium hydroxide until the entire skeletal template was visible (approximately 2-4 hours). Once the skeleton was visible, embryos were placed in KOH: glycerin solutions for 1 hour each (80:20, 60:40, 40:60, and 20:60). Embryos were then stored in 70% glycerol/ 30% PBS.

Whole Mount X-gal Staining

Whole mount X-gal staining was used to localize sites of adenoviral infection (Kern et al., 2007). Embryos were harvested, fixed in 4% paraformaldehyde for 40 minutes and washed 3 times 5 minutes each with cold PBS. Embryos were then washed 3 times for 5 minutes each in cold permeabilization buffer (0.02% Na-deoxycholate, 0.01% NP-40 in PBS) and left on a rocker overnight at 4°C in order to minimize background. Embryos were stained with X-gal (Invitrogen) or RedGal (Research Organics) stain (0.1% K-ferricyanide, 0.1% K-ferrocyanide,

0.02% $MgCl_2$, 0.1% X-gal/Red Gal made in dimethyl formamide at 100 mg/.ml in PBS) at 37°C in the dark. The stain (blue or red) was usually visible within 1.5-4 hours. When staining was complete, embryos were post-fixed in 4% paraformaldehyde for no longer than 30 minutes and then stored in 70% ethanol until ready to progress with the embedding procedure the next day.

Statistical Analysis

Pictures of Alcian Blue stained samples were taken using digital photo-microscopy at low power under a dissecting microscope (Olympus SZ-60) using SPOT-RT camera (Diagnostic Instruments) and software. Measurements of interzone area of each sample were taken using Image-J software (NIH) and a Student's t-test performed with significance set at $p<0.05$ (Hudson et al., 2010). Comparison of control un-injected contralateral limbs was used to test the hypothesis of this study which was that there would be an enlargement of interzone space in the adeno-G1 treated limbs.

Immuno-& Histochemical Staining

Sections were dehydrated, embedded in paraffin wax, and sectioned at 7-8 micrometers. Mouse anti-hemaglutinin IgG (H3663, Sigma) was used at 3.3μg/ml (1:100) to detect the C-terminal tag located on the recombinant G1-domain adenovirus. Biotinylated hyaluronic acid binding protein (Cape Cod) at 2.5 μg/ml (1:200) was used to detect hyaluronan and examine impacts of versican G1-domain overexpression on its localization. Double labeling of target molecules was used during staining procedures when possible. Paraformaldehyde-fixed sections were de-waxed and subjected to antigen unmasking using a citric acid formula at high temperature (Biocare Medical decloaking chamber) for 20 minutes (Snow et al., 2005; Hudson et al., 2010). All samples were

then incubated in 0.25U/ml chondroitinase ABC (Sigma) in PBS for at least one hour at 37°C. Sections were blocked with 3% bovine serum albumen and 1% goat serum in PBS for one hour and incubated with primary immunoreagents overnight at 4°C. Sections were washed with PBS and incubated with FITC-conjugated secondary antibodies (Cappel; 1:400) or TexasRed Streptavidin (Vector labs; 1:200) for up to two hours at room temperature. All secondary reagents were diluted in blocking buffer (3% bovine serum albumen and 1 % goat serum in PBS). In order to control for potential non-specific staining of secondary reagents, primary antibodies were omitted from selected sections in each experiment (Appendix B). Sections were washed in PBS and post-fixed in 80% and 50% ethanol 5 minutes each. Sections were re-equilibrated in PBS and mounted in DABCO (Sigma) anti-fading agent (10% 1X PBS, 90% glycerol, 100mg/mL DABCO) to retard fading of fluorescence (Hudson et al., 2010). All sections were stored at 4°C in the dark.

Protein Extractions

Chicks at HH35/36 were harvested and rinsed with PBS and elbow joints were dissected. Injected elbow joints were pooled, placed in separate centrifuge tubes and kept in cold PBS. The same was done with contralateral control elbow joints. A glass mortar and pestle was used to grind the tissue samples in a mixture of protein extraction buffer (M-PER, Thermo Scientific) containing protease inhibitor cocktail (Sigma). This was done separately for each sample pool and supernatant was removed and placed in a new centrifuge tube placed on ice for 30 minutes. Lysates were clarified by centrifugation at 10,000 X g for 10 minutes, supernatants removed, placed in a new tube, and frozen at -80°C until ready for assay. All samples were assayed for protein content using a Micro BCA^{TM} Protein Assay Reagent Kit (Pierce).

Hyaluronan Zymograms

Activity of hyaluronidase within embryonic chick elbow lysates was assayed using hyaluronan zymography. For this study, zymograms were performed at pH 3.7 and 5.0. Samples were normalized for protein content, separated on a 10% SDS polyacrylamide gel containing 0.17 mg/mL hyaluronan (Genzyme, Framingham, MA) and incubated for 1 hour in 0.3% Triton X-100. Gels were incubated overnight at 37°C in 0.1M sodium formate at pH 3.7 or pH 5.0, containing 0.15M NaCl. Once the overnight incubation was complete gels were treated with 1 mg/mL pronase in 20 mM Tris HCL, at a pH of 8.0, for 1 hour. Gels were then stained with Stains All (MP Biomedicals) overnight. Next, the gel was de-stained using distilled water until bands could be visualized and background was reduced. Bands were imaged using the Fluor-S MultiImaging system (BioRad, Chow et al. 2006).

Hyaluronan ELISA

Elbow lysates were prepared from HH35 chicks as above following microinjection with selected adenoviruses. ELISA was performed using a DuoSet Assay Development kit (R&D Systems). Plates were prepared with a coating of diluted Capture Reagent (0.5 µg/mL in PBS), sealed, and left at room temperature overnight. The next day wells were aspirated and washed with kit Wash Buffer (0.05% Tween 20 in PBS at pH 7.2-7.4) three times. Plates were blocked using Block Buffer (5% Tween 20 in PBS, 0.05% NaN_3) and incubated for one hour at room temperature. Another aspiration and wash series was performed three more times and protein samples were added to wells diluted in the Reagent Diluent (5% Tween 20 in PBS) and incubated for a total of two hours at room temperature. Another wash series was performed as above and Detection

Reagent (0.4µg/mL biotinylated recombinant human aggrecan in Reagent Diluent) was added and incubated at room temperature for another two hours. Wells were aspirated, washed again and Streptavidin-HRP was added to wells and incubated for 20 minutes at room temperature in the dark. Substrate Solution (1:1 ratio of color reagent A-hydrogen peroxide and color reagent B-tetramethylbenzidine) was added to each well after another wash and incubated for 20 minutes at room temperature in the dark. Stop Solution (2N H_2SO_4) was added to each well and optical density determined using a microplate reader (Multiskan Ascent V1.25, Thermo Electron Corporation) at 450 nm and 540 nm. Readings at 540 nm were subtracted from the readings at 450 nm in order to accommodate any optical imperfections on the microplates. To determine hyaluronan concentrations, a hyaluronan standard was analyzed and concentrations were determined based on the equation provided by the standard on a logarithmic chart as suggested by the protocol.

RT-PCR

Microinjections were performed as stated above and embryos harvested at HH35 (embryonic day 9-9.5). Injections assayed were as follows: adeno-G1, co-injection of 4MU & G1, co-injection of hyal2 adeno-shRNA 702 & 1130, and co-injection of DN-CD44 & G1 adenoviruses, and an un-injected contralateral control. RNA was extracted from elbow regions of injected limbs using the RiboPure Kit (Applied Biosystems). Reverse transcription was performed using oligodT priming of sample RNA using the Superscript III First Strand Synthesis Kit (Invitrogen). The cDNA was normalized to equal concentration and used in RT-PCR. All RT-PCR reactions were carried out in a total of 15 µL containing 1µL of Forward and Reverse primers for Hyal-2, and β-actin at 30µM, 1 µL cDNA template (1µL of ddH_2O was used for negative controls), 4.5µL of ddH_2O,

and 7.5µL of MasterMix. RT-PCR was performed in a thermocycler (Bio-Rad MyCycler) for 30 cycles with initial denaturation set at 95°C for 5 minutes, a second denaturation step set at 95°C for 30 seconds, annealing step set at optimal annealing temperature of 49°C for 30 seconds, and elongation step at 72°C for 45 seconds. Once cycles were completed another final elongation step was performed at 72°C for 10 minutes and amplicons held at 4°C. Products were analyzed on a 0.8% agarose gel using gel electrophoresis. Once the gel mixture was prepared and allowed to cool, 2 µL of ethidium bromide was added before pouring the mixture into a gel tray. Gels were electrophoresed for approximately 30 minutes at 135 V and viewed on an ultraviolet transilluminator to observe bands. Primers yielding amplicons of the predicted size (107 base pairs) were then used for real-time PCR.

qRT-PCR of Hyal-2

Based on RT-PCR results, the primer set used was HYAL2 F: 5'-CCTGGACTTCAGCGTCT-3', R: 5'-TGTAGTAGGGGTAGAGCC-3'. As a control, β-actin primers were used to amplify endogenous β-actin in samples (F: 5'-CACAGATCATGTTTGAGACCTT-3', R: 5'-CATCACAATACCAGTGGTACG-3'; Accession #L08165; DeBoever et al., 2008). Reactions were carried out in a total volume of 10 µL and consisted of 1µL of the forward and reverse primers, 1µL cDNA template (1 µL of ddH_2O was used for negative controls), 2µL ddH_2O, and 5 µL of 2X SensiFAST SYBR No-ROX Mix (BIOLINE). The qRT-PCR was carried out in a thermocycler (CFX96 Real-Time System, BioRad) for 41 cycles with the initial denaturation step at 95°C for 2 minutes, a second denaturation step at 95°C for 5 seconds, an annealing step at the optimal temperature of 49°C for 10 seconds, an elongation step at 72°C for 10 seconds, and an additional elongation step at 65°C for 5 seconds. Three technical replicates were tested for

each adenoviral treatment indicated previously with two biological replicates represented due to low embryonic viability. Threshold cycle data was analyzed relative to control samples using MS excel, and Pfaffl (2001) analysis was used for relative quantification calculation. Student's t-test was also performed to determine statistical significance of results.

3. RESULTS

This study was undertaken to provide new information regarding the role of the G1 domain of versican and its interaction with hyaluronan during synovial joint formation, especially within the elbow interzone since there is still little known regarding ECM regulation of interzone dynamics. Recent studies showed that inhibition of versican expression within the developing chick joint led to decreases in interzone area (Nagchowdhuri et al. 2012) and that hyaluronan is crucial to the development of the synovial joint, especially in terms of spacing (Matsumoto et al. 2009). Based on these reports, the present study hypothesized that there would be an overall enlargement of interzone area in developing wing joints injected with recombinant versican G1-domain adenovirus in the presumptive joint region, resulting in alteration of elbow formation due to increased levels of versican-hyaluronan interaction.

Morphological effects in response to adenoviral-mediated overexpression of G1-versican domain in joints were gauged by whole mount staining of limbs using Alcian Blue histochemistry in concert with staining for the adeno-β-galactosidase reporter to aid localization of infected tissues. Histological examination of tissue sections and hyaluronan localization in regions of hemaglutinin-tagged G1 domain expression were used to evaluate effects of adeno-G1 mediated over-expression on joint morphogenesis with higher resolution.

Because recent microarray and real-time PCR experiments in our lab documented upregulation of Hyal-2 transcripts in response to G1-versican overexpression in developing joints, another aim of this study was to assess function and G1-mediated regulation of Hyal-2 during the process of joint morphogenesis in the developing chick embryo. This study investigated versican G1-mediated signaling in order to determine if effects on Hyal-2 were dependent on hyaluronan and/or CD44. In order to study these effects, presumptive joints were

treated with 4-methylumbelliferone and adeno-versican G1 followed by assay for changes in Hyal-2 mRNA via qRT-PCR. This was also tested by injecting embryonic limbs with a dominant negative-CD44 virus to block wild-type CD44-hyaluronan interactions in the presence of versican G1 over-expression. This study also sought to determine if a G1-mediated increase in Hyal-2 mRNA was reflected as an increase in hyaluronidase activity and if this activity was affected by a difference in pH using protein lysates of control and versican G1-treated chick elbow joints. Another method to investigate hyaluronidase function was knock-down of chick Hyal-2 using adeno-shRNAs to examine differences in activity and subsequent hyaluronan loss.

Histochemical/Immunocytochemical Staining

To identify the location of adenoviral infection, whole mount β-galactosidase staining was performed. Recombinant G1 in limbs that were injected with the adeno-G1 versican was immunolocalized with a C-terminal murine hemaglutinin tag. Co-distribution of β-galactosidase staining along with G1-hemaglutinin tag expression was used as a reliable indicator of infection sites. Biotinylated hyaluronan binding protein (bHABP) was used to localize endogenous hyaluronan in the chick elbow joint at HH35/36 and to observe changes in hyaluronan in response to G1 domain overexpression. Distinct pericellular hyaluronan within the developing joint was co-localized with adeno-G1 versican positive chondrocytes within forming articular cartilage areas in both adeno-G1 treated limbs and in limbs treated with 4-methylumbelliferone in conjunction with adeno-G1 versican (Figure 1 and 2). Hyaluronan staining appeared to have a more robust pericellular coat in areas where adeno-G1 was present. In samples treated with adeno-G1 there was a noticeable increase in hyaluronan accumulation within the injected limb versus the contralateral control (Figure 1). In limbs treated with both 4-methylumbelliferone and

adeno-G1 there was a slight decrease in overall hyaluronan accumulation in comparison to the untreated contralateral control limbs (Figure 2).

Whole Mount Alcian Blue Staining

To observe morphological effects of versican G1-domain manipulation, whole mount Alcian blue staining was performed and area measurements were taken of the interzone space between epiphyseal ends of the humerus, ulna, and radius using ImageJ software (Figure 3). Measurements were analyzed using Student's t-test and overall data included averages of measurements from different embryo samples, standard deviations, and p-values of the interzone area of un-injected contralateral control limbs in comparison to the injected limbs (Table 1). There was an average increase of 23% in interzone area (space between humerus, ulna, and radius) resulting from infection with adeno-G1 versican in comparison to contralateral control (un-injected) limbs. Treatment with 4-methylumbelliferone in conjunction with adeno-G1 versican resulted in an average increase of 23% of the interzone dimensions as well. DN-CD44 adenoviral infection resulted in an increase of 41% interzone area. Infection with DN-CD44 in conjunction with adeno-G1 versican resulted in an increase in interzone spacing but results were not significant, however sample size was small due to lack of overall embryonic viability as a result of these co-injections. Results from co-injection of the hyal2 shRNA viruses (702 &1130) resulted in slightly increased spacing, but also insignificant. The original hypothesis that G1-versican overexpression would cause enlargement in the interzone was supported. Differences between contralateral control and injected limbs of adeno-G1 versican alone, co-injection of G1-versican with 4-MU, and DN-CD44 adenovirus were significant at $p<0.05$. Approximately 50% of adeno-G1 versican and 4-MU/G1-versican treated embryos that were viable post-injection

contained a measurable increase in interzone area. Approximately 86% of DN-CD44 treated embryos resulted in an increase in interzone area as well (Table 2).

Hyaluronan ELISA

To determine differences in concentration of hyaluronan between different adenoviral treatments, hyaluronan ELISA was performed on protein lysates of chick elbow joints at HH35 and concentrations were determined using the hyaluronan standard provided with the Duo Kit. Although results were not significant based on Student's t-test, trends were noticed among different samples (Figure 4). Lower levels of hyaluronan were found in embryonic limbs treated with 4-methylumbelliferone in conjunction with adeno-G1 versican in comparison to controls. Higher levels of hyaluronan were found in samples that were treated with adeno-DN-CD44 in addition to adeno-G1 versican. No major differences in hyaluronan concentration were noticed in treatments with Hyal-2 shRNAs, adeno-G1, and adeno-DN-CD44 treatment alone.

Real-Time PCR

To observe changes in HYAL2 gene expression, RT-PCR and qRT-PCR were performed. Primers were checked using RT-PCR and once optimal temperatures and appropriate band sizes were verified they were used in qRT-PCR. Samples assayed included untreated control, 4-methylumbelliferone co-injected with the adeno-G1, adeno-G1 alone, DN-CD44 co-injected with the adeno-G1, and the two Hyal-2 shRNA adenoviruses (Figure 5). Fold change calculations were based on Pfaffl (2001) and provided a means of normalizing all data to the β-actin reference gene. All primers had a 100% efficiency based on the calculation using the formula $E=10^{(-1/slope)}$ (Higuchi et al., 1993). To determine significance of results a Student's t-test

was performed. Results were insignificant based on p-values but trends were visible among different samples. Four-methylumbelliferone in conjunction with the adeno-G1 versican showed a decrease in the relative fold change in comparison to untreated controls. Adeno-DN-CD44 in conjunction with adeno-G1 versican as well as adeno-G1 versican injected alone showed a slight increase in fold change in comparison to untreated controls. The two Hyal-2 shRNA adenoviruses were deemed unsuccessful in terms of ability to knockdown Hyal-2 levels due to the insignificant fold changes in Hyal-2 expression.

Hyaluronan Zymography

To investigate hyaluronidase activity and attempt to correlate that to Hyaluronidase-2 expression, hyaluronan zymograms were performed. Protein lysates of equal concentration from chick elbow joints at HH35 were used in this assay. Based on preliminary results, hyaluronidase activity was seen at 64 kD at pH 3.7. No activity was found approaching the more neutral pH of 5.0 (Figure 6). No major differences in band intensities were seen in samples that were assayed.

Figure 1. Immunohistochemical staining of sagittal sections of HH35 chick elbows in un-injected control (A, C, E) and 5 days following adenoviral treatment with G1-versican (B, D, F, G). Panel B shows G1-hemaglutinin tag localization within the infected chick limb. More intense pericellular hyaluronan staining is noted in areas with G1-hemaglutinin tagged cells (arrows) relative to uninfected-cells showing pericellular hyaluronan staining (D). Panel F shows areas of infection indicated by β-galactosidase staining. Panel G is an overlay of the double-labeled hemaglutinin-tagged adeno- G1 versican and hyaluronan binding protein staining to further accentuate co-localization of hyaluronan-positive cells with sites of infection. Increased interzone spacing consistent with whole mount staining of G1-infected limbs can also be distinguished within the infected limb in comparison to the contralateral control along with increased hyaluronan staining overall (depicted by bracket). Scale bar = 50μM for all panels. h, humerus. u, ulna.

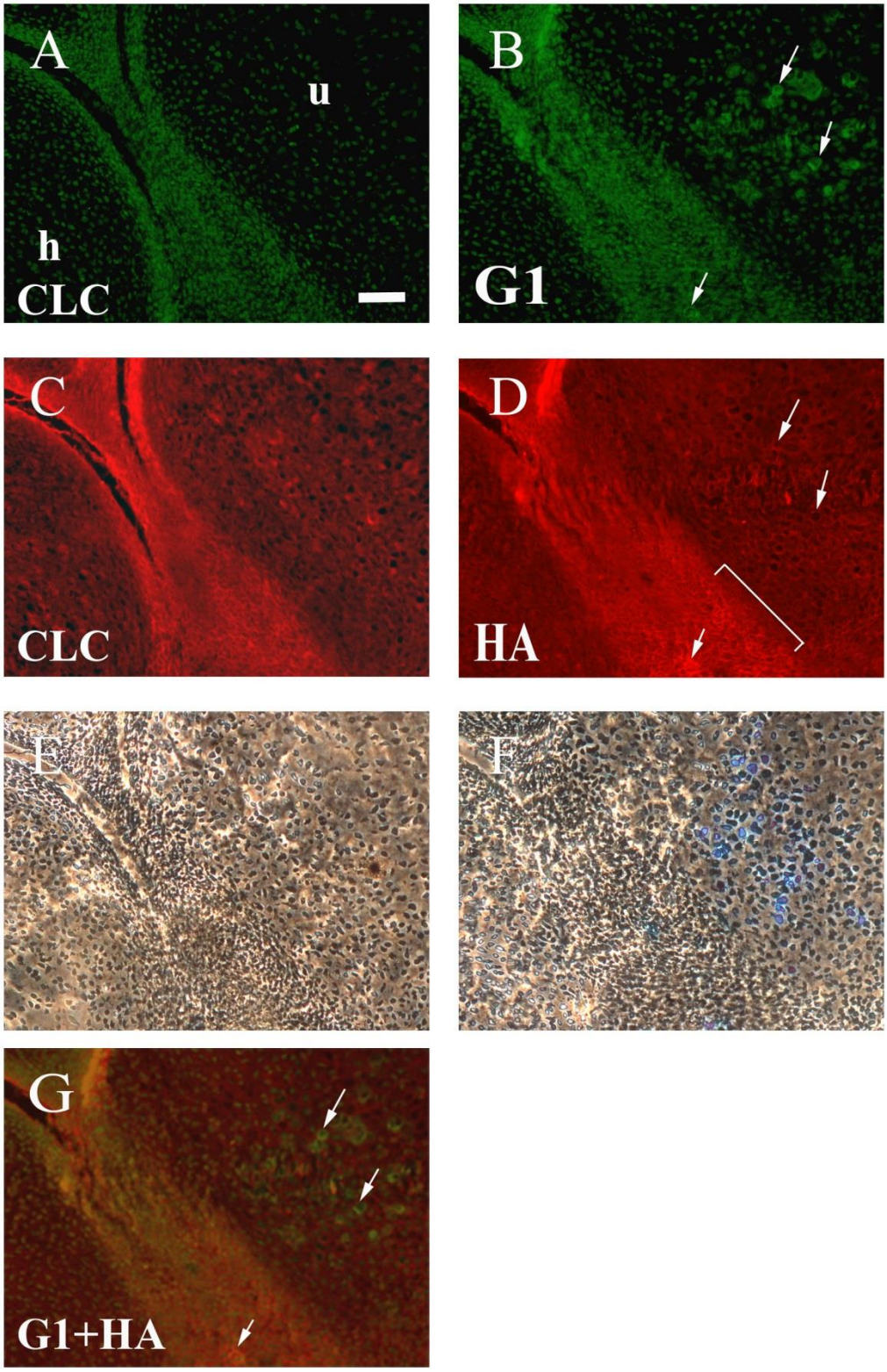
A
u
h
CLC
B
G1
C
CLC
D
HA
E
F
G
G1+HA

Figure 2. Immunohistochemical staining of sagittal sections of chick elbows at HH36 in contralateral control (A, C, E) and following infection with adeno-G1 versican in conjunction with 4-methylumbelliferone at HH25 (B, D, F). Panel B indicates areas of hemaglutinin-tagged G1 cells within developing articular cartilage of the ulna (arrow). Panel D shows pericellular hyaluronan binding protein staining that is more robust in areas with G1-positive cells (arrow). Panels E and F are respective phase contrast images. An intense overall staining of hyaluronan was noticed in the contralateral control limb in comparison to the injected, depicted by large arrows (C, D). Scale bar = 50μM for all images. h, humerus. u, ulna.

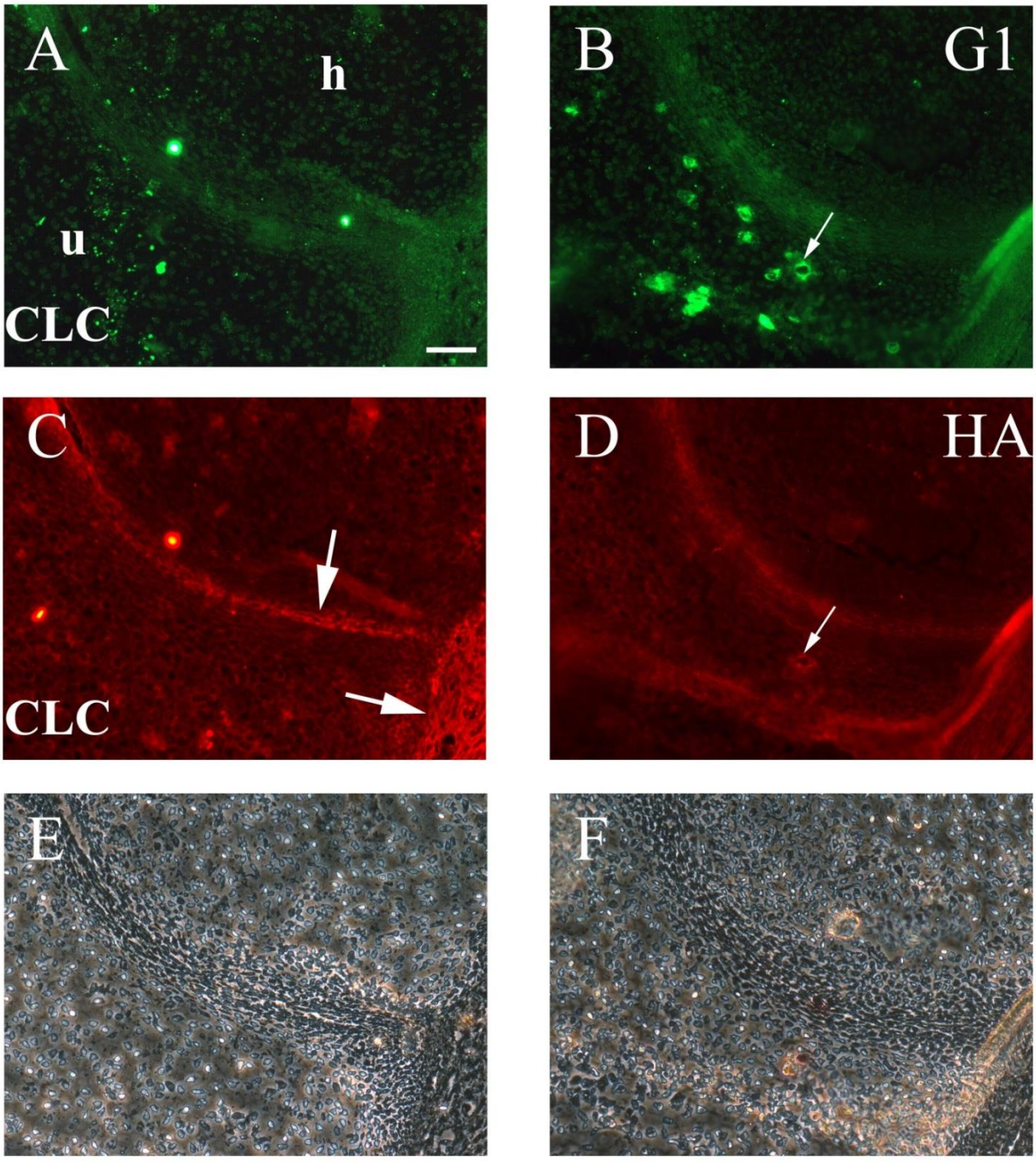
A
h
u
CLC
B
G1
C
CLC
D
HA
E
F

Figure 3. Whole mount Alcian Blue staining of HH35/36 chick limbs depicting results of overexpression of adeno-G1 versican (A), adeno-G1 versican in conjunction with 4-methylumbelliferone (B), and adenoviral infection with DN-CD44 (C). Treatments resulted in an increase in interzone space between epiphyseal ends of the humerus, ulna, and radius in comparison to contralateral controls (CLC). Red staining seen in panel C shows β-galactosidase staining indicating area of adenoviral infection. Panel D depicts how measurements were taken with ImageJ software. All scale bars = 1.0 mm.

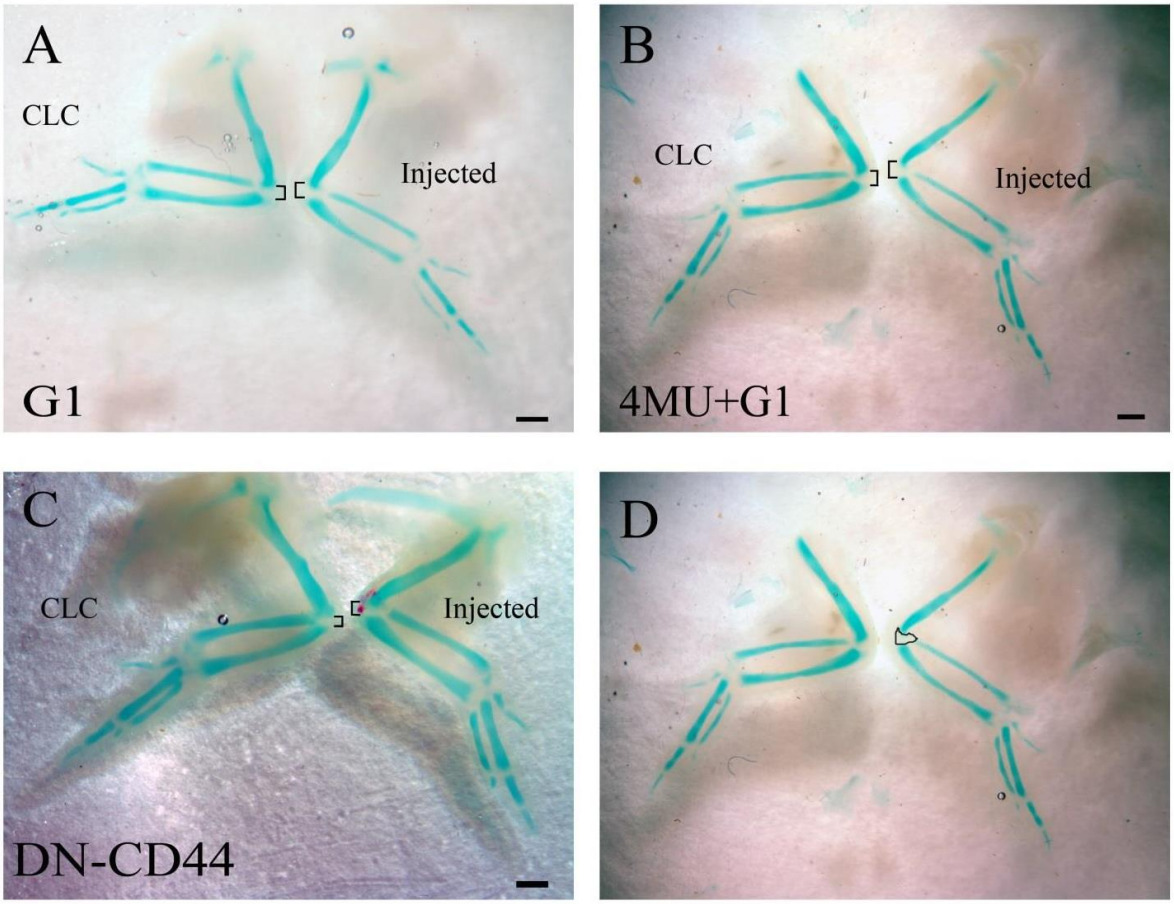

Figure 4. Hyaluronan ELISA assay results. Hyaluronan concentration was determined from absorbances and extrapolated from a standard curve. Statistical analysis was performed using Student's t-test. All results were deemed insignificant ($p>0.05$).

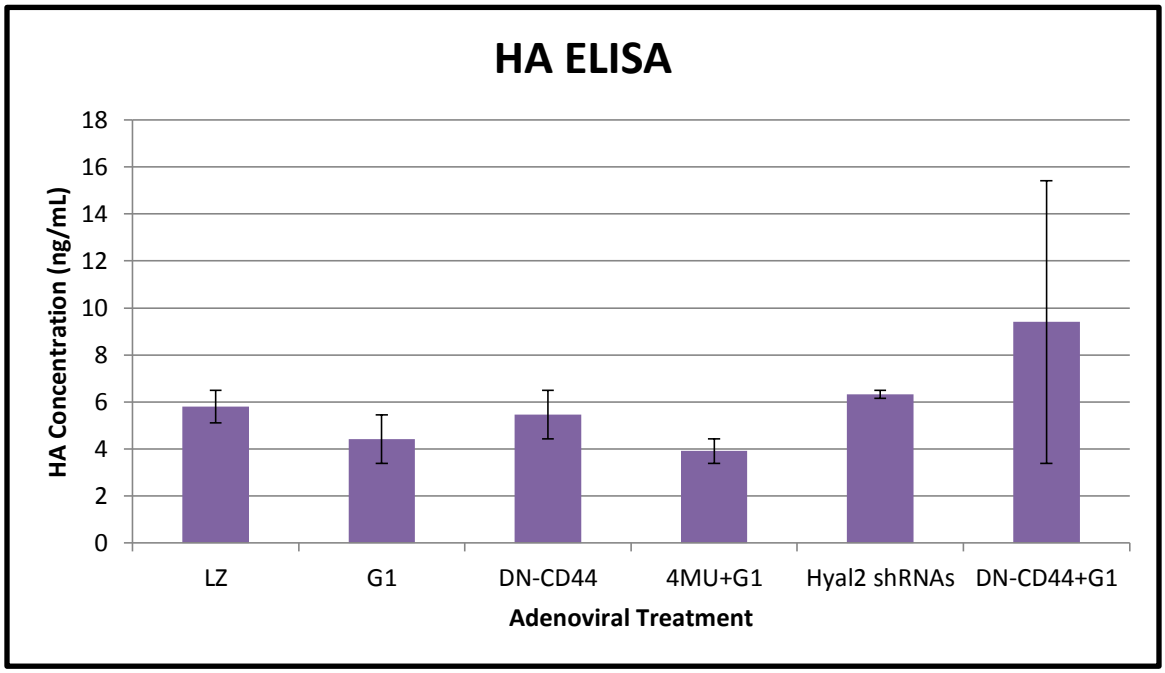

Figure 5. Gene expression results of the Hyal-2 gene normalized with β-actin. Calculations were based on Pflaffl (2001) and statistical significance determined by Student's t-test. All results were deemed insignificant ($p>0.05$).

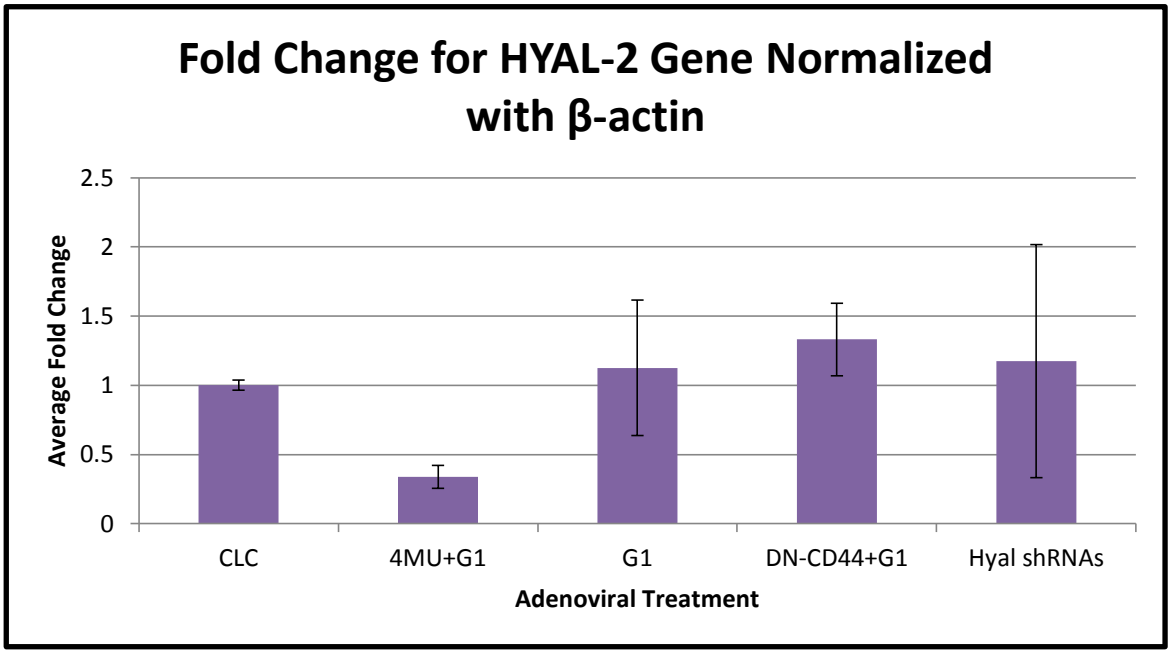

Figure 6. Hyaluronan zymography results. Top image depicts hyaluronidase activity at pH 3.7. Bottom image depicts the lack of hyaluronidase activity approaching the more neutral pH of 5.0. Hyaluronidase activity bands were seen at approximately 64 kD, the molecular weight of Hyal-2.

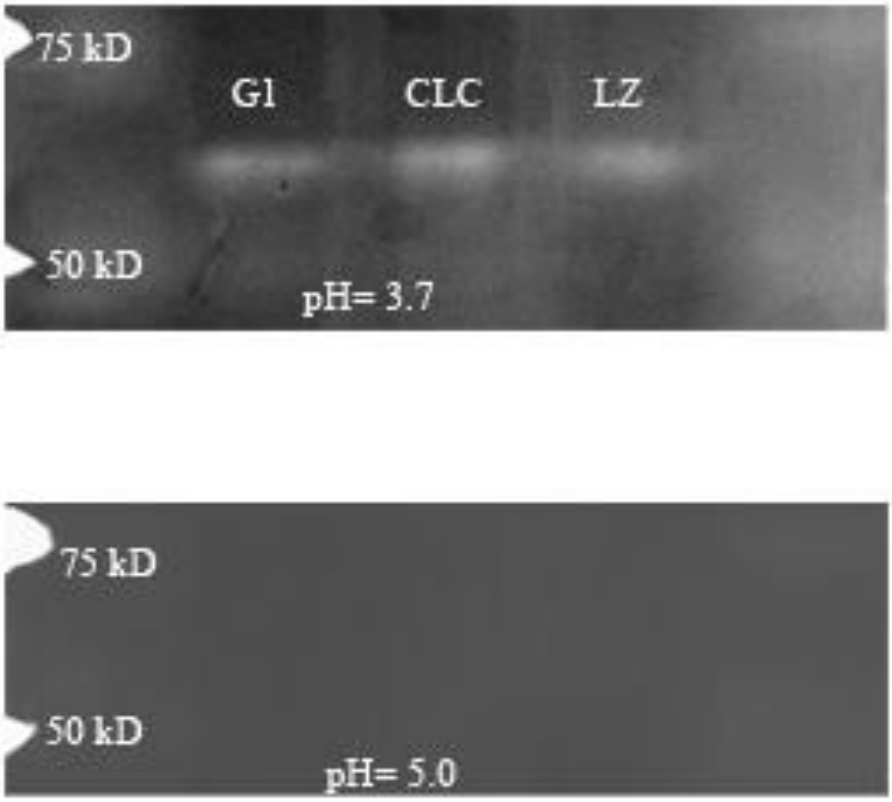

Table 1. Estimates of chick embryo interzone areas in square-millimeters from Alcian Blue whole mount staining at HH35/36 following treatment at HH25. Mean matched-pair analysis was used to determine whether differences between average interzone area measurements of injected and contralateral control wings were statistically significant. *P-values < 0.05 were determined significant.

Adenovirus(es) Injected	Number of Viable Embryos at HH35/36 Post-Injection (n)	CLC Interzone Area (mm^2)	Injected Interzone Area (mm^2)	% Increase in Interzone Area	P-value
G1	8	0.094 ± 0.02	0.122 ± 0.02	23%	0.00017*
DN-CD44	6	0.091 ± 0.03	0.153 ± 0.03	41%	0.0017*
4MU+G1	3	0.124 ± 0.01	0.162 ±0.01	23%	0.012*
DN-CD44+G1	3	0.124 ± 0.01	0.161 ± 0.03	13%	0.159
Hyal shRNA 702+1130	3	0.097 ± 0.02	0.112 ± 0.01	23%	0.143

Table 2. Chick elbow joint phenotypes shown by morphological assessment of Alcian Blue whole mount staining at HH35/36 injected with G1-adeno versican, DN-CD44 adenovirus, and 4-methylumbelliferone in conjunction with G1-adeno versican at HH25.

Adenovirus(es) Injected	Number of Viable Embryos Post-Injection	Number of Viable Embryos with Increased Interzone Areas	Percent of Viable Embryos with Phenotype
G1	16	8	50%
DN-CD44	7	6	86%
4MU+G1	6	3	50%

4. DISCUSSION

Synovial joint formation is prefaced by the formation of the interzone, an area consisting of three layers that will create the articular cartilage and fluid-filled space of the synovial cavity (Ito and Kida, 2000; Guo et al. 2004; Pacifici et al., 2005). Versican, a chondroitin sulfate proteoglycan found within the extracellular matrix has been shown to participate in limb morphogenesis and is primarily localized within the interzone of the developing joint following initial chondrogenesis (Shepard et al. 2007). There has been recent evidence that individual domains of versican can function independently of the intact proteoglycan (Kern et al., 2007; Hudson et al., 2010). A recent study in the early stage murine interzone localized a proteolyzed versican fragment containing the G1 domain of versican that was co-distributed with the intact proteoglycan, ADAMTS-1, and hyaluronan (Capehart 2010). Localization of this proteolyzed fragment, DPEAAE (the neoepitope sequence resulting from cleavage of versican by ADAMTS-1), showed that the G1 domain can be freed from the intact proteoglycan and may participate in further synovial joint formation (Capehart 2010).

The purpose of this study was to investigate the function of the G1 domain of versican and, in addition, determine how G1 overexpression within the developing joint leads to upregulation of Hyaluronidase-2 as noted in previous microarray and qRT work from the lab. Specifically, we wanted to distinguish if effects of G1 versican overexpression on Hyal-2 were dependent on hyaluronan or its major cell receptor, CD44, since both have been identified as playing roles in synovial joint formation (Craig et al., 1990; Archer et al., 1994; Edwards et al. 1994; Pitsillides et al. 1995; Dowthwaite et al., 1998; Matsumoto et al., 2009). Previous work showed that versican interacts with hyaluronan and CD44, and all are localized within the developing joint (Wu et al., 2005). To study versican interaction with the hyaluronan pathway,

replication deficient adenoviruses overexpressing the G1 domain of versican or a DN-CD44 adenovirus, along with 4-methylumbelliferone (a hyaluronan synthesis inhibitor) were injected into the presumptive joint space of chick embryos at HH25 and joints analyzed at HH35/36.

Versican has been shown in several studies to play a critical role in joint development. When versican levels were knocked down within the developing chick synovial joint, a decreased interzone area was noticed along with decreased hyaluronan expression in adeno-infected locations (Nagchowdhuri et al., 2012). Conditional versican knockout within a mouse model resulted in formation of limbs shortened in length and joints described as tilted (Choocheep et al., 2010). When we overexpressed the G1 domain of versican in developing synovial joints we were able to distinguish a phenotype in whole mount samples consisting of a significantly enlarged interzone area in comparison to controls (Figure 3, Table 1). When hyaluronan expression was observed in sagittal sections of adeno-G1 infected chick limbs it was found that in areas with hemaglutinin-tagged recombinant G1, there was also more intense pericellular hyaluronan staining (Figure 1). This co-localization of adeno-G1 along with intense bHABP staining was also seen in a study that overexpressed the G1 domain within humeral primordia (Hudson et al., 2010). Since hyaluronan has been shown to help establish and maintain spaces (Pratt et al., 1975; Pitsillides et al., 1995), this increased hyaluronan accumulation in the presence of adeno-G1 provides an explanation for the increased interzone area seen within whole mount adenoviral treated limbs suggesting that endogenous versican proteolytic fragments containing the G1 domain (Capehart 2010) may interact with hyaluronan to increase cell spacing during joint formation. Previous work in the lab has demonstrated that overexpression of G1 versican causes significant upregulation of hyaluronan pathway genes, including Hyal-2. Microarray data revealed an average 2.5 fold increase in Hyal-2 expression in the G1 treated

joint in comparison to controls and real-time PCR data revealed an approximate 2 fold upregulation of Hyal-2 in samples which overexpressed G1 versican (Vick 2012). Real-time PCR was performed on samples in the present study and although results were deemed insignificant, possibly due to small sample size or masking due to inclusion of RNA from surrounding tissues, a trend of increased Hyal-2 expression was seen in G1-treated joints in comparison to controls.

Another necessity for synovial joint development is hyaluronan; knockout of HAS2, a hyaluronan synthase, in a mouse model resulted in extremely deformed limbs and absence or malformation of joints (Matsumoto et al., 2009). To assess hyaluronan's possible role in G1-mediated upregulation of Hyal-2, 4-methylumbelliferone was co-injected with the adeno-G1. Other studies have also utilized 4-methylumbelliferone to inhibit hyaluronan synthesis; a recent study using 4-methylumbelliferone in porcine trabecular meshwork cells recorded decreased hyaluronan synthesis and hyaluronan accumulation as seen in both ELISA and HABP staining (Keller et al., 2012). When 4-methylumbelliferone was co-injected with adeno-G1, chick limb sections and hyaluronan ELISA both revealed a decrease in overall hyaluronan accumulation in treated limbs in comparison to un-injected contralateral controls which is consistent with studies mentioned above. In areas where the adeno-G1 hemaglutinin tag was present, however, more intense hyaluronan staining was also seen as with adeno-G1 treatment alone, suggesting that the G1 versican is still capable of binding and retaining hyaluronan to a visible degree following treatment with 4-methylumbelliferone. Interestingly, whole mount data showed an increase in joint interzone spacing of limbs treated with 4-methylumbelliferone in conjunction with adeno-G1 although there also appeared to be thinning of cartilage structures in the injected limbs, particularly in proximity to the targeted joint areas. Hyaluronan plays a major role in the

structural unit of cartilage (Sherman et al., 1994) and this decrease in overall hyaluronan accumulation and increased interzone area suggests that there could be disrupted cartilage formation causing diminished epiphyseal ends of the humerus, radius, and ulna which could account for increased spacing within the interzone. Real-time PCR results indicated a decrease in Hyal-2 expression in samples treated with 4-methylumbelliferone in conjunction with adeno-G1. This decrease in Hyal-2 expression alongside decreased hyaluronan accumulation seen in both the ELISA and bHABP staining results suggests that hyaluronan is necessary for G1-mediated upregulation of Hyal-2. Since results above indicate that G1-mediated signaling may be dependent on hyaluronan, it was important to also determine if CD44, a hyaluronan receptor, was playing a role in Hyal-2 upregulation.

CD44 has been shown to bind, mediate internalization, and regulate degradation of hyaluronan (Knudson et al., 1993). In samples treated with DN-CD44 adenovirus alone, which likely blocks wild-type CD44-hyaluronan interactions, an increase in interzone area was also seen which suggests that levels of hyaluronan were increased within the interzone due to inability to be internalized by wild-type CD44 (Jiang et al., 2002). A similar result was seen in a study involving transgenic mice lacking detectable CD44 within skin keratinocytes and corneal epithelium; in response to the decrease in CD44 there was a large increase in hyaluronan accumulation since it was not able to be bound and internalized (Kaya et al., 1997). Unfortunately, due to low viability of treated embryos, histochemical analysis of hyaluronan changes as a result of DN-CD44 or adeno-DN-CD44 and G1 co-injection expression was not able to be accomplished in the present study and should be examined further in the future.

Real time PCR revealed little change in Hyal-2 expression in response to adeno-DN-CD44 in conjunction with adeno-G1 suggesting that CD44 does not have a role in G1-mediated

upregulation of Hyal-2. Whole mount samples that were treated with both adeno-G1 versican and DN-CD44 had a slight but insignificant increase in overall interzone area. Although insignificant, hyaluronan ELISA of adeno-G1 in conjunction with adeno-DN-CD44 revealed a trend of increased hyaluronan accumulation in joint tissue lysates which may provide an explanation for the increased interzone area seen in whole mounts. The hyaluronan ELISA trend suggests that G1-hyaluronan binding in addition to the inability of hyaluronan to be internalized by endogenous wild-type CD44 in the presence of DN-CD44 (Jiang et al., 2002) could cause more hyaluronan retention within the pericellular matrix. Moreover, there could be binding of hyaluronan to lower affinity receptors (such as the tailless CD44) present in the joint interzone when hyaluronan is bound to G1-versican. In a study of hyaluronan and cell surface CD44 in the presence of another hyaluronan binding protein, TSG-6 (tumor necrosis factor stimulated gene-6 protein) it was found that if hyaluronan bound TSG-6 it was then capable of binding lower affinity receptors including a tailless form of CD44 (Lesley et al., 2004) very similar to the DN-CD44 used in our study. Lesley's results are consistent with results from the present study suggesting that hyaluronan may bind DN-CD44 (tailless form) whenever G1 is bound to hyaluronan which would cause increased hyaluronan accumulation in the developing joint. Alternatively, recent *in situ* hybridization analysis in our lab has identified another putative CD44 receptor within the interzone area, Sushi domain containing 5 (Susd5) located in carpal and elbow joints of the developing chick limb (Robins 2013). Although function of Susd5 is unknown, it has a link domain similar to versican and CD44 capable of binding hyaluronan (Brissett et al., 1996; Vicent et al., 2008) and may represent a lower affinity receptor capable of binding hyaluronan-G1 versican potentially leading to a signaling cascade resulting in Hyal-2

upregulation. This possibility needs to be investigated in future studies in order to make definitive conclusions.

In conclusion, during joint development the G1 domain of versican can be freed from the intact proteoglycan and may have a role in furthering joint development (Hudson et al., 2010; Capehart 2010). This G1 domain can bind and interact with hyaluronan and is capable of upregulating hyaluronan pathway genes when overexpressed within the developing chick joint. The decreased Hyal-2 expression in the presence of adeno-G1 in conjunction with 4-methylumbelliferone suggests that G1-mediated signaling to upregulate Hyal-2 is dependent on the presence of hyaluronan. Based on preliminary results from this study, CD44 does not appear necessary for G1-mediated upregulation of Hyal-2. Further research needs to follow with CD44 knockdown in combination with G1 overexpression in order to arrive at a definitive conclusion regarding its necessity for Hyal-2 upregulation and its effects on hyaluronan expression.

5. REFERENCES

Ang LC, Zhang Y, Cao L, Yang BL, Young B, Kiani C, Lee V, Allan K, Yang BB. (1999). Versican enhances locomotion of astrocytoma cells and reduces cell adhesion through its G1 domain. *J Neuropathol Exp Neurol, 58,* 597-605.

Archer CW, Morrison H, Pitsillides AA. (1994). Cellular aspects of the development of diarthrodial joints and articular cartilage. *J. Anat, 184*, 447-456.

Bajorath J, Greenfield B, Munro SB, Day AJ, Aruffo A. (1998). Identification of CD44 residues important for hyaluronan binding and delineation of the binding site. *J. Biol. Che,. 273*, 338-343.

Bell DM, Leung KKH, Wheatley SC, Ng LJ, Zhou S, Ling KW, Sham MH, Koopman P, Tam PPL, Cheah KSE. (1997). SOX9 directly regulates the type-II collagen gene. *Nature Genetics, 16*, 174-178.

Bode-Lesniewska B., Dours-Zimmermann M. T., Odermatt B. F., Briner J., Heitz P. U., and Zimmermann D. R. (1996). Distribution of the large aggregating proteoglycan versican in adult human tissues. *J Histochem Cytochem, 44*, 303-312.

Brissett NC, Perkins SJ. (1996). The protein fold of the hyaluronate-binding proteoglycan tandem repeat domain of link protein, aggrecan and CD44 is similar to that of the C-type lectin superfamily. *FEBS letters, 388*(2), 211-216.

Capehart AA. (2010). Proteolytic cleavage of versican during limb joint development. *Anat Rec, 293*, 208-214.

Choocheep K., Hatano S., Takagi H., Watanabe H., Kimata K., Kongtawelert P., Watanabe H. (2010). Versican facilitates chondrocyte differentiation and regulates joint morphogenesis. *J Biol Chem, 285*, 21114-21125.

Chow G, Knudson W. (2005). Characterization of promoter elements of the human HYAL-2 gene. *J Biol Chem, 29*, 26904-26912.

Chow G, Knudson CB, Knudson W. (2006). Expression and cellular localization of human hyaluronidase-2 in articular chondrocytes and cultured cell lines. *Osteoarthritis Cartilage, 9*, 849-858.

Craig FM., Bentley G., Archer CW. (1987). The temporal and spatial patterns of collagen I and II and keratan sulfate in developing chick MTP joint. *Development, 99*, 383-391.

Craig FM, Bayliss MT, Bentley G, Archer CW. (1990). A role for hyaluronan in joint development. *J. Anat, 171*, 17-23.

Csoka AB, Scherer SW, Stern R. (1999). Expression analysis of six paralogous human hyaluronidase genes clustered on chromosomes 3p21 and 7q31. *Genomics, 60*, 356-361.

Csoka AB, Frost GI, Stern R. (2001). The six hyaluronidase-like genes in the human and mouse genomes. *Matrix Biol, 20*, 499-508.

Dowthwaite GP, Edwards JCW, Pitsillides AA. (1998). An essential role for the interaction of hyaluronan and hyaluronan-binding proteins during joint development. *J. Histochem. Cytochem, 46*, 641-651.

Dowthwaite GP, Flannery CR, Flannelly J, Lewthwaite JC, Archer CW, Pitsillides AA. (2003). A mechanism underlying the movement requirement for synovial joint cavitation. *Matrix Biology, 22*, 311-322.

Edwards JCW, Wilkinson LS, Jones HM, Soothill P, Henderson KJ, Worrall JG, Pitsillides AA. (1994). The formation of human synovial joint cavities: a possible role for hyaluronan and CD44 in altered interzone cohesion. *J. Anat, 185*, 355-367.

Flannery CR, Little CB, Hughes CE, Caterson B. (1998). Expression and activity of articular cartilage hyaluronidases. *Biochem and Biophy Res Commun, 251*, 824-829.

Foster JW, Dominguez-Steglich MA, Guioli S, Kwok C, Weller PA, Weissenbach J, Mansour S, Young ID, Goodfellow PN, Brook JD, Schafer AJ. (1994). Campomeloc dysplasia and autosomal sex reversal caused by mutations in an SRY-related gene. *Nature, 372*, 525-530.

Hall BK, Miyake T. (1992). The membranous skeleton: the role of cell condensations in vertebrate skeletogenesis. *Anat Embryol (Berl), 186*, 107-124.

Hall BK, Miyake T. (2000). All for one and one for all: condensations and the initiation of skeletal development. *Bioessays, 22*, 138-147.

Hamburger V, Hamilton HL. (1951). A series of normal stages in the development of the chick embryo. *J. Morphol, 88*, 49-92.

Hardingham TE, Muir H. (1972). The specific interaction of hyaluronic acid with cartilage proteoglycans. *Biochim Biophys Acta, 279*, 401-405.

Higuchi R, Fockler C, Dollinger G, Watson R. (1993). Kinetic PCR analysis: real-time monitoring of DNA amplification reactions. *Biotechnology, 11*, 1026-1030.

Hua Q, Knudson CB, Knudson W. (1993). Internalization of hyaluronan by chondrocytes occurs via receptor-mediated endocytosis. *J. Cell Science, 106*, 365-375.

Hudson KS, Andrews K, Early J, Mjaatvedt CH, Capehart AA. (2010). Versican G1 domain and V3 isoform overexpression results in increased chondrogenesis in the developing chick limb in ovo. *Anat Rec, 293*(10), 1669-1678.

Isacke, CM. (1994). The role of cytoplasmic domain in regulating CD44 function. *J. Cell Sci, 107*, 2353-2359.

Isacke, CM, Yarwood H. (2002). Molecules in focus: The hyaluronan receptor, CD44. *J. Biochem. & Cell Bio, 34*, 718-721.

Ito MM, Kida My. (2000). Morphological and biochemical re-evaluation of the process of cavitation in the rat knee joint: cellular and cell strata alterations in the interzone. *J Anat, 197*, 659-679.

Jiang H, Peterson RS, Wang W, Bartnik E, Knudson CB, Knudson W. (2002). A requirement for the CD44 cytoplasmic domain for hyaluronan binding, pericellular matrix assembly, and receptor-mediated endocytosis in COS-7 cells. *J. Biol. Chem. 277*, 10531-10538.

Kamiya N, Watanabe H, Habuchi H, Takagi H, Shinomura T, Shimizu K, Kimata K. (2006). Versican/PG-M regulates chondrogenesis as an extracellular matrix molecule crucial for mesenchymal condensation. *J Biol Chem, 281*, 2390-2400.

Kaya G, Rodriguez I, Jorcano JL, Vassalli P, Stamenkovic I. (1997). Selective suppression of CD44 in keratinocytes of mice bearing an antisense CD44 transgene driven by a tissue-specific promoter disrupts hyaluronate metabolism in the skin and impairs keratinocyte proliferation. *Genes Devel, 11*, 996-1007.

Kuczuk MH, Scott WJ. (1984). Potentiation of acetazolamide induced ectrodactyly in SwV and C57bL/6J mice by cadmium sulfate. *Teratology, 29*, 427–435.

Keller KE, Sun YY, Vranka JA, Hayashi L, Acott TS. (2012). Inhibition of hyaluronan synthesis reduces versican and fibronectin levels in trabecular meshwork cells. *PLoS One, 7*(11), e48523.

Kern CB, Norris RA, Thompson RP, Argraves WS, Fairey SE, Reyes L, Hoffman S, Markwald RR, Mjaatvedt CH. (2007). Versican proteolysis mediates myocardial regression during outflow tract development. *Dev Dyn, 236*, 671-683.

Kimata K, Oike Y, Tani K, et al. (1986). A large chondroitin sulfate proteoglycan (PG-M) synthesized before chondrogenesis in the limb bud of chick embryo. *J Biol Chem, 261*, 13517-13525.

Knudson CB, Toole BP. (1985). Changes in the pericellular matrix during differentiation of limb bud mesoderm. *Developmental Biology, 112*, 308-318.

Knudson W, Bartnik E, Knudson CB. (1993). Assembly of pericellular matrices by COS-7 cells transfected with CD44 homing receptor genes. *Proc. Natl. Acad. Sci, 90*, 4003-4007.

Knudson CB, Knudson W. (2001). Cartilage proteoglycans. *Cell & Dev. Biol, 12*, 69-78.

Knudson CB. (2003). Hyaluronan and CD44: Strategic players for cell-matrix interaction during chondrogenesis and matrix assembly. *Birth Defects Research, 69*, 174-196.

Knudson W, Chow G, Knudson CB. (2002). CD44-mediated uptake and degradation of hyaluronan. *Matrix Biology, 21*, 15-23.

Kultti A, Pasonen-Seppanen S, Jauhiainen M, Rilla KJ, Karna R, Pyoria E, Tammi R, Tammi M. (2009). 4-Methylumbelliferone inhibits hyaluronan synthesis by depletion of cellular UDP-glucuronic acid and downregulation of hyaluronan synthase 2 and 3. *Exp. Cell. Res, 315*, 1914-1923.

Laurent TC. (1989). The biology of hyaluronan. Introduction. *Ciba Found. Symp, 143*, 1-20.

Lepperdinger G, Strobl B, Kreil G. (1998). HYAL2, a human gene expressed in many cells, encodes a lysosomal hyaluronidase with a novel type of specificity. *J Biol Chem, 273*, 22466-22470.

Lepperdinger G, Mullegger J, Kreil G. (2001). Hyal2-less active, but more versatile? *Matrix Biology, 20*, 509-514.

Lesley J, Gál I, Mahoney DJ, Cordell MR, Rugg MS, Hyman R, Day AJ, Mikecz K. (2004). TSG-6 modulates the interaction between hyaluronan and cell surface CD44. *J Biol Chem, 279*, 25745-25754.

Li Y, Toole BP, Dealy CN, Kosher RA. (2007). Hyaluronan in limb morphogenesis. *Dev. Biol, 305*, 411-420.

Liu D, Sy M-S. (1996). A cysteine residue located in the transmembrane domain of CD44 is important in binding of CD44 to hyaluronic acid. *J. Exp. Med, 183*, 1987-1994.

Matsumoto K, Shionyu M, Go M, Shimizu K, Shinomura T, Kimata K, Watanabe H. (2003). Distinct interaction of versican/PG-M with hyaluronan and link protein. *J Biol Chem, 278*, 41205-41212.

Matsumoto K, Li Y, Jakuba C, Sugiyama Y, Sayo T, Okuno M, Dealy CN, Toole BP, Takeda J, Yamaguchi Y, Kosher RA. (2009). Conditional inactivation of Has2 reveals a crucial role for hyaluronan in skeletal growth, patterning, chondrocyte maturation and joint formation in the developing limb. *Development, 136*(16), 2825-2835.

Nagchowdhuri PS, Andrews KN, Robart S, Capehart AA. (2012). Versican knockdown reduces interzone area during early stages of synovial joint development. *Anat Rec, 295*(3), 397-409.

Naor D, Nedvetzki S. (2003). CD44 in rheumatoid arthritis. *Arthritis Res Ther, 5*, 105-115.

Ng LJ, Wheatley S, Muscat GEO, Conway-Campbell J, Bowles J, Wright E, Bell D, Tam PPL, Cheah KSE, Koopman P. (1997). Sox9 binds DNA, activates transcription, and coexpresses with type II collagen during chondrogenesis in the mouse. *Developmental Biology, 183*, 108-121.

Neufeld EF, Sando GN, Garvin AJ, Rome LH. (1977). The transport of lysosomal enzymes. *J Supramol. Struct, 6*, 95-101.

Orkin RW, Toole BP. (1980a). Isolation and characterization of hyaluronidase from cultures of chick embryo skin- and muscle-derived fibroblasts. *J Biol Chem, 255*, 1036-1042.

Orkin RW, Toole BP. (1980b). Chick embryo fibroblasts produce two forms of hyaluronidase. *J Cell Bio, 85*, 248-257.

Oster GF, Murray JD, Maini PK. (1985). A model for chondrogenic condensations in the developing limb: the role of extracellular matrix and cell tractions. *J. Embryol. Exp. Morphol, 89*, 93-112.

Pacifici M, Koyama E, Iwamoto M. (2005). Mechanisms of synovial joint and articular cartilage formation: recent advances, but many lingering mysteries. *Birth Defects Res, 75,* 237-248.

Pfaffl MW. (2001). A new mathematical model for relative quantification in real-time RT-PCR. *Nucleic Acids Research, 29*, 2002-2007.

Pitsillides AA, Archer CW, Prehm P, Bayliss MT, Edwards JC. (1995). Alterations in hyaluronan synthesis during developing joint cavitation. *J. Histochem, 43*, 263-273.

Pratt RM, Larsen MA, Johnston MC. (1975). Migration of cranial neural crest cells in a cell-free hyaluronate-rich matrix. *Dev. Biol, 44,* 298-305.

Robins JE. (2013). Spatial expression of matrix and matrix receptor proteins in the developing synovial joint. Department of Biology. East Carolina University.

Shambaugh J, Elmer A. (1980). Analysis of glycosaminoglycans during chondrogenesis of normal and brachypod mouse limb mesenchyme. *J. Embryol. Exp. Morphol, 56*, 225-238.

Shepard JB, Gliga DA, Morrow AP, Hoffman S, Capehart AA. (2008). Versican knock-down compromises chondrogenesis in the embryonic chick limb. *Anat Rec, 291*, 19-27.

Shepard JB, Krug HA, LaFoon BA, Hoffman S, Capehart AA. (2007). Versican expression during synovial joint morphogenesis. *Int J Biol Sci, 3*, 380-384

Sherman L, Sleeman J, Herrlich P, Ponta H. (1994). Hyaluronante receptors: key players in growth, differentiation, migration and tumor progression. *Current Opinion in Cell Biology, 6*, 726-733.

Shinomura T, Jensen KL, Yamagata M, Kimata K, Solursh M. (1990). The distribution of mesenchyme proteoglycan (PG-M) during wing bud outgrowth. *Anat Embryol (Berl), 181*, 227-233.

ShinomuraT, Nishida Y, Ito K, Kimata K. (1993). DNA cloning of PG-M, a large chondroitin sulfate proteoglycan expressed during chondrogenesis in chick limb buds. Alternative spliced multiforms of PG-M and their relationship to versican. *J Biol Chem, 268*, 14461-14469.

Snow HE, Riccio LM, Hoffman S, Mjaatvedt CH, Capehart AA. (2005). Versican expression during skeletal/joint morphogenesis and patterning of muscle and nerve in the embryonic mouse limb. *Anat Rec, 282*, 95-105.

Stern R. (2003). Devising a pathway for hyaluronan catabolism: are we there yet? *Glycobiology, 13*, 105-115.

Toole BP. (1972). Hyaluronate turnover during chondrogenesis in the developing chick limb and axial skeleton. *Dev. Biol, 29,* 321-329.

Toole BP. (1991). Glycosaminoglycans in morphogenesis. Cell Biology of the *Extracellular Matrix*, 259-294.

Vick SR. (2012). Validation of candidate genes in response to versican manipulation in developing synovial joints. Department of Biology. East Carolina University.

Vicent S, Luis-Ravelo D, Antón I, García-Tuñon I, Borrás-Cuesta F, Dotor J, De Las Rivas J, Lecanda F. (2008). A novel lung cancer signature mediates metastatic bone colonization by a dual mechanism. *Cancer Res, 68*(7), 2275-2285.

Wagner T, Wirth J, Meyer J, Zabel B, Held M, Zimmer J, Passantes J, Bricarelli FD, Keutel J, Hustert E, Wolf U, Tommerup N, Schempp W, Scherer G. (1994). Autosomal sex reversal and campomelic dysplasia are caused by mutations in and around the SRY-related gene SOX9. *Cell, 79*(6), 1111-1120.

Williams DR, Presar AR, Richmond AT, Mjaatvedt CH, Hoffman S, Capehart AA. (2005). Limb chondrogenesis is compromised in the versican deficient *hdf* mouse. *Biochem Biophys Res Comm, 334*, 960-966.

Wu Y, La Pierre Dp, Wu J, Yee AJ, Yang BB. (2005). The interaction of versican with its binding partners. *Cell Research, 15*, 483-494.

Yamagata M, Suzuki S, Akiyama SK, Yamada KM, Kimata K. (1989). Regulation of cell-substrate adhesion by proteoglycans immobilized on extracellular substrates. *J Biol Chem, 264*, 8012-8018.

Yang BL, Zhang Y, Cao L, Yang BB. (1999). Cell adhesion and proliferation mediated through the G1 domain of versican. *J Cell Biochem, 72*, 210-220.

Yoshioka Y, Kozawa E, Urakawa H, Arai E, Futamura N, Zhuo L, Kimata K, Ishiguro N, Nishida Y. (2013). Suppression of hyaluronan synthesis alleviates inflammatory responses in murine arthritis and in human rheumatoid synovial fibroblasts. *Arthritis & Rheumatism, 65*(5), 1160-1170.

Zako M, Shinomura T, Ujita M, Ito K, Kimata K. (1995). Expression of PG-M (V3), an alternatively spliced form of PG-M without a chondroitin sulfate attachment region in mouse and human tissues. *J Biol Chem, 270*, 3914-3918.

Zhang Y, Cao L, Kiana C, Yang BL, Hu W, Yang BB. (1999). Promotion of chondrocyte proliferation by versican mediated by G1 domain and EGF-like motifs. *J Cell Biochem, 73*, 445-457.

Zhang Y, Cao L, Kiana CG, Yang BL, Yang BB. (1998). The G3 domain of versican inhibits mesenchymal chondrogenesis via the epidermal growth factor-like motifs. *J Biol Chem, 273*, 33054-33063.

Zhang Y, Wu Y, Cao L, Lee V, Chen L, Lin Z, Kiani C, Adams ME, Yang BB. (2001). Versican modulates embryonic chondrocyte morphology via the epidermal growth factor-like motifs in G3. *Exp Cell Res, 263*, 33-42.

Zimmerman DR, Ruoslahti E. (1989). Multiple domains of the large fibroblast proteoglycan, versican. *Embo J, 8*, 2975-2981.

Appendix A: Animal Care and Use Committee Forms

East Carolina University

Animal Care and Use Commitee
212 Ed Warren Life Sciences Building
East Carolina University
Greenville, NC 27834

252-744-2436 office
252-744-2355 fax

February 14, 2011

Anthony Capehart, Ph.D.
Department of Biology
Howell Science Complex
East Carolina University

Dear Dr. Capehart:

Your Animal Use Protocol entitled, "Hyaluronidase, a Hydrolase that Contributes to the Formation of Limb Joints during Embryonic Development and the Destruction of Joints in Adults with Osteoarthritis" (AUP #D258) was reviewed by this institution's Animal Care and Use Committee on 2/14/11. The following action was taken by the Committee:

"Approved as submitted"

Please contact Dale Aycock at 744-2997 prior to hazard use

A copy is enclosed for your laboratory files. Please be reminded that all animal procedures must be conducted as described in the approved Animal Use Protocol. Modifications of these procedures cannot be performed without prior approval of the ACUC. The Animal Welfare Act and Public Health Service Guidelines require the ACUC to suspend activities not in accordance with approved procedures and report such activities to the responsible University Official (Vice Chancellor for Health Sciences or Vice Chancellor for Academic Affairs) and appropriate federal Agencies.

Sincerely yours,

Scott E. Gordon, Ph.D.
Chairman, Animal Care and Use Committee

SEG/jd

enclosure

East Carolina University

Animal Care and Use Commitee
212 Ed Warren Life Sciences Building
East Carolina University
Greenville, NC 27834

252-744-2436 office
252-744-2355 fax

January 9, 2012

Anthony Capehart, Ph.D.
Department of Biology
Howell Science Complex
East Carolina University

Dear Dr. Capehart:

Your Animal Use Protocol entitled, "Versican G1 Domain and Hyaluronan Interaction in Synovial Joint Morphogenesis" (AUP #D269) was reviewed by this institution's Animal Care and Use Committee on 1/09/12. The following action was taken by the Committee:

"Approved as submitted"

Please contact Dale Aycock at 744-2997 prior to hazard use

A copy is enclosed for your laboratory files. Please be reminded that all animal procedures must be conducted as described in the approved Animal Use Protocol. Modifications of these procedures cannot be performed without prior approval of the ACUC. The Animal Welfare Act and Public Health Service Guidelines require the ACUC to suspend activities not in accordance with approved procedures and report such activities to the responsible University Official (Vice Chancellor for Health Sciences or Vice Chancellor for Academic Affairs) and appropriate federal Agencies.

Sincerely yours,

Scott E. Gordon, Ph.D.
Chairman, Animal Care and Use Committee

SEG/jd

enclosure

Appendix B: Representative Secondary Controls

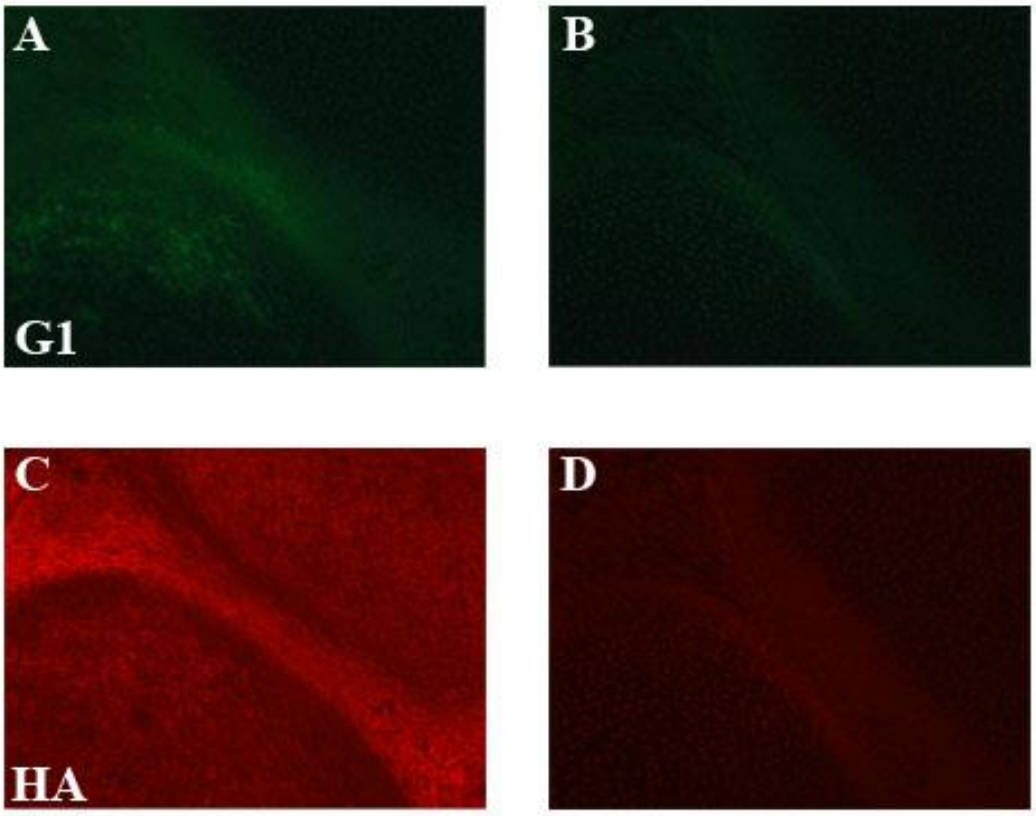

Sections stained with HA-7 primary antibody along with bHABP showed hemaglutinin-tagged adeno-G1 (A) and pericellular hyaluronan staining (C). Sections that were stained without a primary antibody showed minimal fluorescence when stained with goat, anti-mouse IgG FITC-conjugated antibody (B) or TexasRed Streptavidin (D).